Toward Understanding the Structural Basis of Cyclin-Dependent Kinase 6 Specific Inhibition

Heshu Lu[†] and Ursula Schulze-Gahmen*[,‡]

Physical Biosciences Division at Lawrence Berkeley National Laboratory, 1 Cyclotron Road, MS3, Berkeley, California

Received January 12, 2006

Cyclin-dependent kinases (CDKs) are key players in cell cycle control, and genetic alterations of CDKs and their regulators have been linked to a variety of cancers. Hence, CDKs are obvious targets for therapeutic intervention in various proliferative diseases, including cancer. To date, drug design efforts have mostly focused on CDK2 because methods for crystallization of its inhibitor complexes have been well established. CDK4 and CDK6, however, may be at least as important as enzymes for cell cycle regulation and could provide alternative treatment options. We describe here two complex structures of human CDK6 with a very specific kinase inhibitor, PD0332991, which is based on a pyrido[2,3-*d*]pyrimidin-7-one scaffold, and with the less specific aminopurvalanol inhibitor. Analysis of the structures suggests that relatively small conformational differences between CDK2 and CDK6 in the hinge region are contributing to the inhibitor specificity by inducing changes in the inhibitor orientation that lead to sterical clashes in CDK2 but not CDK6. These complex structures provide valuable insights for the future development of CDK-specific inhibitors.

Introduction

Cyclin-dependent kinases (CDKs) play a central role in cell cycle control. The high incidence of genetic alterations of CDKs and their regulators in a number of cancers make CDKs an important target for therapeutic intervention in various proliferative diseases, including cancer.[1] Hence, considerable efforts were made to screen for and design CDK-specific inhibitors. To date, a large number of chemically diverse inhibitors with high affinities for CDK1, CDK2, and CDK5 are available and several of them have entered clinical trials to treat cancer.[2−4] Drug design of CDK2-specific inhibitors was greatly helped by the high-resolution X-ray structures of CDK2 and its inhibitor complexes. Biochemical evidence suggests that CDK4−cyclinD and CDK6−cyclinD complexes are at least as important as CDK2 for regulating cell proliferation.[5−7] Progression through the G1/S phase requires phosphorylation of the retinoblastoma (Rb) protein by CDK4[8,9] or the highly homologous enzyme CDK6[9,10] in complex with their activating subunits, the D-type cyclins. Hyperphosphorylation of Rb diminishes its ability to repress gene transcription through the E2 family of transcription factors and consequently allows synthesis of protein products necessary for DNA replication. Thus, the catalytic activity of CDK4 and CDK6 (CDK4/6) regulates a critical checkpoint for the G1/S transition and the commitment to cell divisions.

More than 90% of human tumors abandon the control mechanisms for this transition point through a variety of genetic and biochemical adaptations.[5,11] Examples of these abnormalities include up-regulation of CDK4 itself, amplification of the D-type cyclins, down-regulation of a naturally occurring inhibitor of CDK4 and CDK6 (called $p16^{INK4}$), and deletion or mutation of Rb itself.[11−14] All of these aberrations can lead to loss of proliferative controls either through elimination of the checkpoint altogether or through inappropriate or enhanced CDK4/6 activity resulting in hyperphosphorylation of Rb. The frequency of these aberrations clearly implies that abrogation of the G1 checkpoint or acceleration of the CDK4−cyclinD and CDK6−cyclinD pathways provides distinct advantages to cancer cells in terms of proliferation and perhaps survival. Hence, selective inhibitors for CDK4/6 might be valuable compounds for the treatment of cancer or other proliferative diseases.

In recent years, a few CDK4/6 selective inhibitors have been described in the literature. These include semispecific inhibitors, such as a triaminopyrimidine derivative, CINK4,[15] and carbazoles,[15] and more specific high-affinity inhibitors with a pyrido-[2,3-*d*]pyrimidin-7-one template.[16−18] The structural basis for the high specificity of the latter inhibitors is unknown because a three-dimensional structure of CDK4 is still missing and only one crystal structure of a CDK6−inhibitor complex with a nonspecific inhibitor, fisetin, has been published.[19] We report here the crystal structures of human CDK6, activated by binding a viral cyclin from herpesvirus saimiri (Vcyclin), in complex with two chemical inhibitors, aminopurvalanol,[20] a fairly unspecific inhibitor, and PD0332991, a pyrido[2,3-*d*]pyrimidin-7-one inhibitor with high specificity for CDK4 and CDK6.[18] Analysis of the structures suggests that relatively small conformational differences between CDK2 and CDK6 in the hinge region are responsible for the inhibitor specificity by inducing small changes in the inhibitor orientation that may lead to sterical clashes in only some types of CDK enzymes.

Results and Discussion

Structure Description. The X-ray structures of CDK6−Vcyclin in complex with the inhibitors PD0332991 and aminopurvalanol (Figure 1) were determined to 3.0 and 2.8 Å, respectively. The complex crystals grow in the same space group with similar cell dimensions as the crystals of the unliganded CDK6−Vcyclin complex.[21] They refined to *R* values of 22.9% (R_{free} = 30.6%) for PD0332991 and 23.8% (R_{free} = 30.1%) for aminopurvalanol with good geometry (Table 1). Electron density maps showed clear density for both inhibitors in the ATP binding pocket between the N-terminal and C-terminal domains of CDK6 (Figure 2). After the inhibitors were built into the ATP binding pocket of CDK6, intermolecular contacts between

* To whom correspondence should be addressed. Phone: 510 486-5854. Fax: (510) 486-6059. E-mail: uschulze-gahmen@lbl.gov.

[†] Current address: Department of Molecular and Cell Biology, University of California, Berkeley.

[‡] Physical Biosciences Division at Lawrence Berkeley National Laboratory.

10.1021/jm0600388 CCC: $33.50
Published on Web 05/28/2006

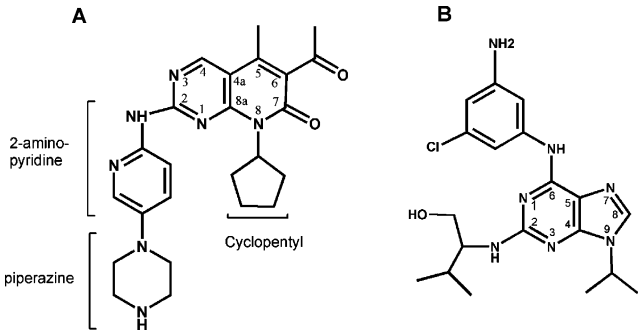

Figure 1. Molecular structures of PD0332991 (A) and aminopurvalanol (B).

Table 1. Statistics for Data Collection and Refinement of CDK6−Vcyclin Complexes

parameter	PD0332991	aminopurvalanol
	data collection	
space group	$P6_522$	$P6_522$
cell dimensions (Å)	$a = b = 71.15$	$a = b = 71.52$
	$c = 446.88$	$c = 449.30$
resolution range (Å)	50−3.0	50.0−2.8
no. of observations	92 005	143 129
no. of unique reflections	13 633	17 833
completeness (%)[a]	93.0 (63.3)	96.8 (99.5)
average $I/\sigma(I)$ [a]	35.3 (3.1)	15.4 (3.8)
R_{sym} (%)[a,b]	4.9 (33.4)	9.0 (44.8)
mosaicity	0.50	0.75
	refinement	
resolution (Å)	20−3.0	20.0−2.8
no. of reflections	12 886	16 516
R_{cryst}[c]/R_{free}[d]	0.229/0.306	0.238/0.301
no. of atoms	4085	4061
CDK6	2134	2121
Vcyclin	1908	1903
PD0332991	33	28
rmsd bond lengths (Å)	0.012	0.011
rmsd bond angles (deg)	1.42	1.37
mean *B*-factor protein (Å^2)	53.3	73.7
mean *B*-factor inhibitor (Å^2)	53.0	80.0
Ramachandran analysis (%)		
most favored[e]	86.2	84.5
additionally allowed	11.2	13.1
generously allowed	2.3	2.2
disallowed	0.2	0.2

[a] Values in parentheses refer to the highest resolution shell. [b] $R_{sym} = \sum_h\sum_i |I_{h,i} - I_h|/\sum_h\sum_i I_{h,i}$ for the intensity (I) of i observation of reflection h. [c] $R_{cryst} = \sum_h ||F_{obs}(h)| - |F_c(h)||/\sum_h|F_{obs}(h)|$ for all data. [d] R_{free} was calculated for 5% of structure factor amplitudes excluded from refinement. [e] Most favored region in Ramachandran plot as defined in PROCHECK.[22]

the ligands and CDK6 were determined with the program CONTACT.[22] The analysis of the intermolecular contacts between CDK6 and the inhibitors in this study is somewhat limited by the relatively low resolution of the complex structures, which makes it more difficult to evaluate the significance of small structural changes. Taking in consideration these limitations, CDK6−inhibitor interactions are discussed in the following paragraphs.

There are a total of 73 contacts shorter than 4.0 Å between PD0332991 and CDK6, including four hydrogen bonds (Figure 3A). The hydrogen bonds from N3 and N2−H to the backbone of Val101 are homologous to those found in all CDK2−inhibitor complexes.[23] Two additional hydrogen bonds between the nitrogen of the aminopyridine side chain and the D102 carbonyl oxygen and between the C6-acetyl group and the peptide amide of D163 orientate the inhibitor in the ATP binding pocket. The C5 and C6 substituents are filling the pocket in front of the gate keeper residue F98 in the back of the ATP binding pocket almost completely, while the piperazinylpyridine substituent in the C2 position is pointing out of the binding pocket toward the so-called specificity region of the binding pocket.[23] The cyclopentyl substituent is binding close to where the ribose of the natural ligand ATP would be expected to bind. The PD0332991 inhibitor appears to fit very tightly into the binding pocket between the N-terminal and C-terminal domain, leaving very little room for even small changes in the binding orientation (Figure 4A).

The inhibitor aminopurvalonol, however, is binding with a less tight fit in the binding pocket (Figure 4B). There are 64 intermolecular contacts between aminopurvalanol and CDK6, of which five are hydrogen bonds (Figure 3). The hydrogen bonds include two conserved bonds with the backbone atoms of V101 and three hydrogen bonds with the 3-amino-5-Cl-anilino substituent of the purine scaffold. These last three hydrogen bonds are probably not very strong because of the partial solvent exposure of the aniline group. In general, most of the hydrogen bonds with the ligand are relatively long, also indicating lower energy contributions by these hydrogen bonds.

Functional Analysis. The IC_{50} values for PD0332991 with CDK4 and CDK6 range between 0.009 and 0.015 μM and are >10 μM for 36 protein kinases tested, with the exception of dual-specificity tyrosine phosphorylation-regulated kinase 1A (2 μM) and mitogen-activated protein kinase-activated protein kinase 1a (8 μM).[18] The inhibitor shows an exceptional high level of specificity for the CDK4/6 subgroup of the CDK family. To identify the structural basis for this high specificity, the CDK6−PD0332991 complex was superimposed onto the CDK2−cyclinA complex with indirubin-5-sulfonate (PDB code 1E9H) using residues 56−67 and 98−163 (CDK6 numbering) for the superposition. These residues were chosen for superposition because they will superimpose CDKs on the structurally more conserved C-terminal kinase domain and on residues in the hinge region and α1 helix that are bordering the ATP binding pocket. After placement of the PD0332991 inhibitor by superposition into the CDK2 binding pocket, its position was further optimized to allow the formation of conserved hydrogen bonds with CDK2 residues 83 and 84, which were observed in the CDK6 complex with PD0332991. Analysis of this CDK2−PD0332991 model identifies several unfavorably short distances between the C5 methyl group and $F80^{CDK2}$ and between the C6-acetyl group and $F80^{CDK2}$ (Figure 5). The short distances of about 3 Å would explain the very low affinity of the inhibitor to CDK2. The sterical clashes are observed in CDK2 but not in CDK6 because of small conformational changes in the hinge region connecting the N-terminal and C-terminal domains. This conformational change makes hydrogen bond formation between PD0332991 and CDK2 residue 83/84 and favorable van der Waals contacts with the gate keeper residue $F80^{CDK2}$ mutually exclusive in the model complex. It is possible that the linker residues in CDK2 are flexible enough to adjust their conformation to allow for PD0332991 binding in the ATP binding pocket. However, the current structural data and the fact that several of the conserved sequence differences between CDK4/6 and other CDKs are located in the hinge region ($H100^{CDK6}$ versus $F82^{CDK2}$) and in structurally adjacent residues ($F39^{CDK6}$ versus $V29^{CDK2}$) raise the possibility that the hinge region conformation is kinase-specific and may be important for the specificity of the PD0332991 inhibitor.

In addition, contacts between the C2 substituent of PD0332991 and residues at the mouth of the ATP binding pocket are affecting inhibitor potency. SAR studies of the C2 substituents showed that replacing the 2-aminopyridinepiperazine by 2-ami-

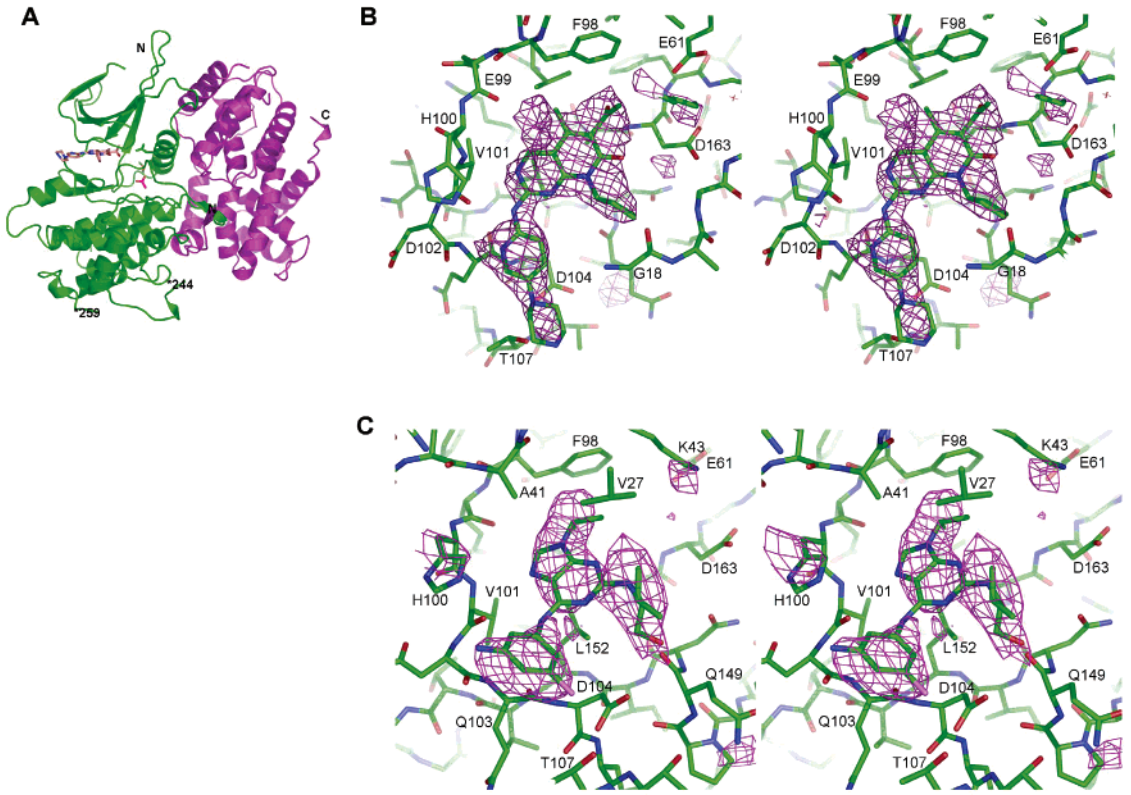

Figure 2. Inhibitor binding to CDK6−Vcyclin. (A) Schematic presentation of the whole CDK6−Vcyclin complex with PD0332991 bound in the cleft between the N-terminal and C-terminal domain of CDK6. (B) Electron density for the bound PD0332991 inhibitor. The $\alpha_{calc}(|F_o| - |F_c|)$ simulated annealing omit map was calculated to 3.0 Å resolution and contoured at 2σ. (C) Electron density for aminopurvalanol bound to CDK6. The $\alpha_{calc}(|F_o| - |F_c|)$ simulated annealing omit map was calculated to 2.8 Å resolution and contoured at 2σ. CDK6 is shown in green and Vcyclin in magenta. Figure 2 was created using the program Pymol.[36]

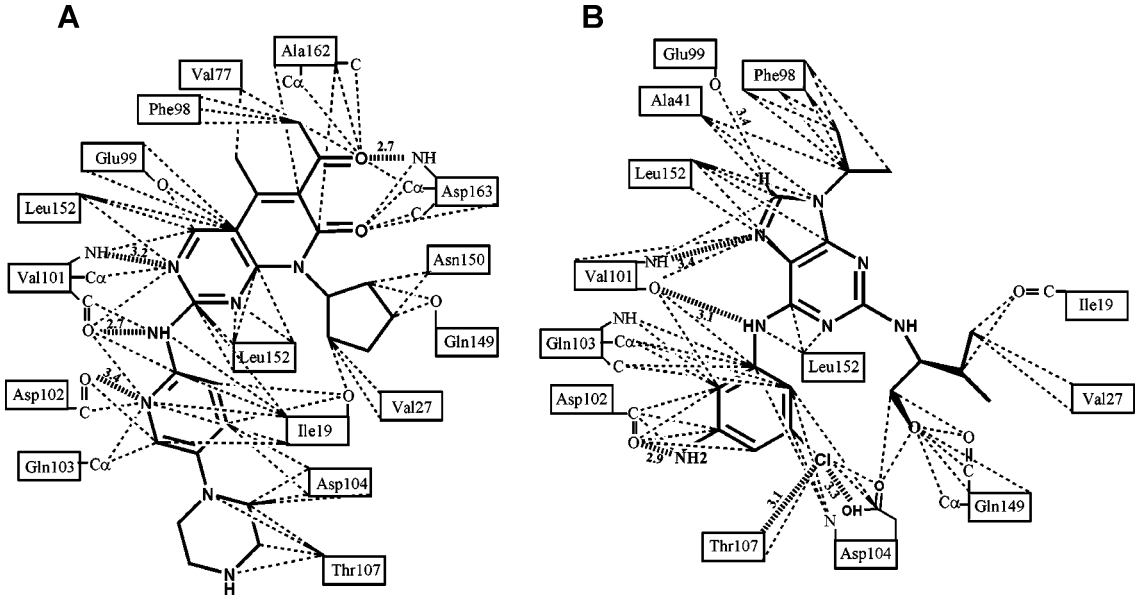

Figure 3. Schematic of CDK6 interactions with PD0332991 (A) and aminopurvalanol (B). Protein residues are shown as rectangular boxes labeled with the residue number. Side chain contacts are indicated by lines connecting to the respective residue box, and interactions to main chain atoms are shown as lines to the specific main chain atoms. van der Waals contacts are indicated as broken lines, and H-bonds are indicated by dashed lines.

nopyridine increases the IC_{50} value for CDK4−cyclinD 40-fold, while the IC_{50} value for CDK2−cyclinA remains above 5 μM for both inhibitors.[16] Replacing the piperazine group of the C2 side chain with a variety of heterocyclic groups, including piperidine, 4-hydroxypiperidine, morpholine, and 3,5-dimethylmorpholine, has little effect on the binding affinity of the inhibitor,[16] suggesting that the presence of a bulky group in this position improves inhibitor potency but does not contribute much to its specificity. The SAR studies agree with the observed weak electron density for the piperazine moiety in the CDK6 complex structure. The piperazine ring is interacting with the side chains of $D104^{CDK6}$ and $T107^{CDK6}$. Distances between the threonine hydroxyl and the piperazine nitrogens are between 3.4 and 3.6 Å, suggesting the possibility of hydrogen bonds

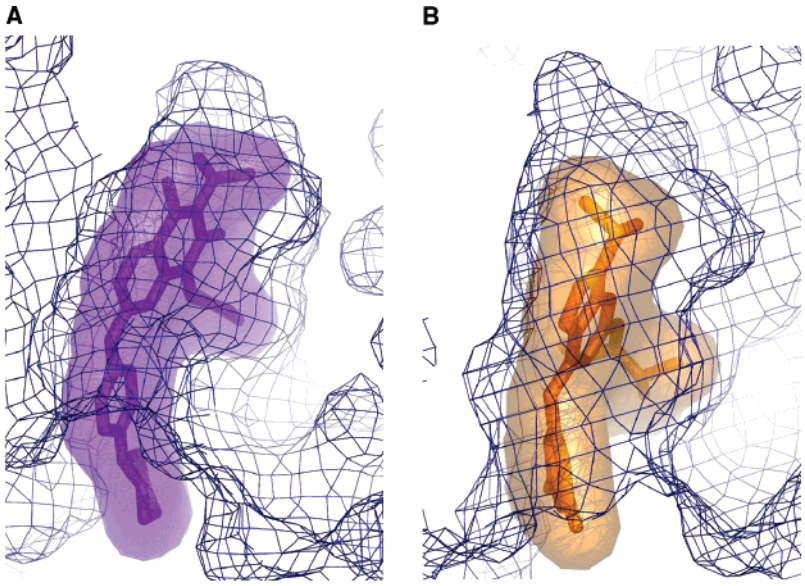

Figure 4. Surface representation of the bound inhibitors and the ligand binding pocket of CDK6. The surfaces of the inhibitors are shown as solid, partially transparent surfaces in magenta for PD0332991 and in yellow for aminopurvalanol. The surface of the CDK6 binding pocket is shown as a blue-lined mesh. Figure 4 was created using the program Pymol.[36]

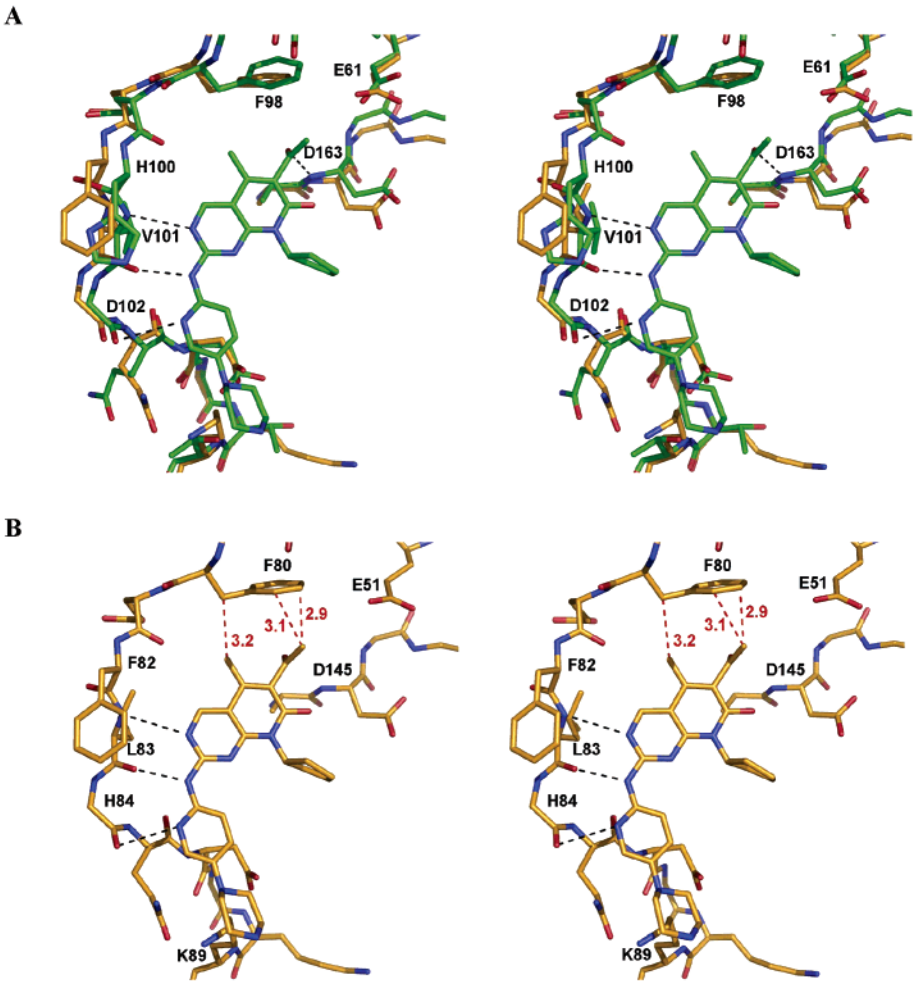

Figure 5. Models of PD0332991 bound to the hinge region of CDK6 and CDK2. (A) The crystal structure of PD0332991 bound to CDK6 is shown in green with the crystal structure of CDK2−CyclinA (PDB code 1E9H) superimposed in yellow. (B) Model of PD0332991 bound to human CDK2. Hydrogen bonds between CDK6 or CDK2 and the inhibitor are drawn as black broken lines. Close contacts between CDK2 and PD0332991 are drawn as red broken lines with distance labels in Å units. The side chains of residues $D102^{CDK6}$ and $H84^{CDK2}$ were omitted for clarity. Figure 5 was created using the program Pymol.[36]

that could not be clearly identified in the 3.0 Å structure. However, the weak density of the piperazine ring would argue against the presence of stabilizing hydrogen bonds between the kinase and inhibitor in this region. $T107^{CDK6}$ is replaced by

lysine in CDK1, CDK2, and CDK5. Analysis of the CDK2−PD0332991 model indicates that replacement of $T107^{CDK6}$ by K89 in CDK2 will most likely not interfere sterically with inhibitor binding because of the flexibility of the lysine side chain. In summary, it appears that the enzyme specificity and potency of PD0332991 are based on steric hindrance in binding the C5 and C6 substituents of the inhibitor molecule in CDK2 versus CDK6 and on interactions of the C2 substituent with protein residues at the mouth of the ATP binding pocket. This is in contrast to reported findings for another CDK4/6 specific inhibitor where SAR and molecular modeling studies indicated that inhibitor interactions with residues in the specificity determining region are most important for inhibitor specificity.[24]

Aminopurvalanol binds with an IC_{50} of 0.45 μM to CDK6−Vcyclin. The IC_{50} values for binding to CDK1−cyclinB, CDK2−cyclinA, and CDK5−p25 are 0.033, 0.033, and 0.02 μM, respectively (L. Meijer, personal communication). Analysis of the CDK6−aminopurvalanol interactions showed that the intermolecular hydrogen bonds were quite long. Attempts to improve the geometry of the hydrogen bonds through small changes in the inhibitor orientation lead to sterical clashes between the substituted aniline group and the backbone of residues 102^{CDK6} and 103^{CDK6} or the side chain of $H100^{CDK6}$. Comparison of the CDK6−aminopurvalanol complex with the related CDK2−purvalanol B complex[25] and with other CDK2−cyclinA structures shows small variations in the hinge region conformation. These small conformational differences together with the side chain substitution of $H100^{CDK6}$ to $F82^{CDK2}$ may cause the observed differences in binding affinity. At the limited resolution of 2.8 Å, it is, however, difficult to pinpoint the exact reason for the different potency of aminopurvalanol toward CDK6 versus CDK1 or CDK2.

Conclusion

Cyclin-dependent kinases are important targets for therapeutic intervention in various proliferative diseases because of their central role in cell cycle control. Most drug design efforts so far have focused on CDK2 because this enzyme is easily crystallized with a variety of inhibitors. Several small-molecule CDK inhibitors are currently in clinical trials, although most of them inhibit multiple CDKs. CDK4 and CDK6 form a subgroup within the CDKs based on sequence alignments and functional differences. They phosphorylate the Rb protein, which is required for progression through the G1/S phase of the cell cycle and the commitment to cell division. The CDK4/6 enzymes may provide a better target for highly specific intervention and regulation of cell cycle progression. To explore the structural basis for inhibitor specificity for CDK4/6, we determined the crystal structures of CDK6−Vcyclin complexes with two small-molecule inhibitors: the highly specific inhibitor PD0332991 and a less specific inhibitor aminopurvalanol. Our results suggest that small conformational differences in the hinge region and an inhibitor molecule that fills the binding pocket nearly completely contribute to the specificity of PD0332991. The hinge region connecting the two kinase domains forms several intermolecular hydrogen bonds with bound inhibitors, which orientate the inhibitor molecule in the binding pocket. Differences in the hinge conformation lead to differences in the inhibitor orientation, causing sterical clashes between parts of the inhibitor and residues lining the ligand binding pocket. In addition, contacts between the C2 substituent of PD0332991 and residues at the mouth of the ATP binding pocket increase inhibitor potency. Our structural results on the CDK6−PD0332991 complex agree well with the previous identification of inhibitor groups critical for CDK4 specificity by structure−activity relationship analyses.[16,26] The information gained from this analysis will be valuable for the future design and improvement of CDK-specific inhibitor molecules.

Experimental Section

Inhibitors. Aminopurvalanol was a gift from Prof. L. Meijer from the C.N.R.S., France. PD0332991 was provided to us by Pfizer Inc. Both inhibitors were dissolved in DMSO to a final concentration of 10 and 25 mM, respectively.

Crystallization and Inhibitor Soaking. A complex of human CDK6 and Vcyclin was expressed and purified from baculovirus-infected SF9 insect cells, as described previously.[27]

CDK6−Vcyclin crystals were grown by the hanging-drop vapor diffusion method at 22 °C. Equal volumes of protein (10 mg/mL protein, 25 mM Tris, pH 8.0, 150 mM NaCl, 10 mM DTT, 0.5 mM EDTA) and well solution (50 mM Tris, pH 8.0, 0.1 M CaOAc, 10−13% PEG 3350, 10 mM DTT) were mixed and suspended over 1 mL of well solution. Sulfobetaine 201 was added to the drop to a final concentration of 0.1 M. Crystals reached a final size of ~0.2 mm × 0.1 mm × 0.1 mm within 3−4 days. Crystals of unliganded CDK6−Vcyclin were soaked with inhibitor by transferring them into a 2 μL sitting-drop well solution of 50 mM Tris, pH 8.0, 15% PEG 3350, 5% glycerol, 150 mM NaCl, 0.1 M CaOAc, 10 mM DTT, and 0.1 M sulfobetaine with 1.25 mM PD0332991 and 5% DMSO or with 1.0 mM aminopurvalanol and 10% DMSO. The drops were equilibrated against the same well solution without inhibitor for 48 h at 22 °C. Crystals were harvested and flash-frozen in a solution composed of the well solution with 20% (v/v) glycerol.

Data Collection. X-ray diffraction data for the PD0332991 and aminopurvalanol complex crystals were collected at beamline 8.2.1 and beamline 5.0.1 at the Advance Light Source (Lawrence Berkeley Laboratories, Berkeley, CA), respectively. For the PD0332991 complex, a total rotation range of 70° was collected, with 0.5° rotation per frame at a distance of 350 mm and a wavelength of 1.0 Å. For the aminopurvalanol complex, a total rotation range of 90° was collected, with 0.5° rotation per frame at a distance of 280 mm and a wavelength of 1.0 Å. The intensities were integrated and scaled using the program HKL2000[28] with final statistics shown in Table 1.

Structure Determination. The initial phases were obtained by molecular replacement with the program AMoRe,[29] using the previously published CDK6−Vcyclin structure (PDB code 1JOW) as a starting model. The initial molecular replacement models had an R factor of 0.344 (R_{free} = 0.347) for the CDK6−Vcyclin−PD0332991 complex and 0.376 (R_{free} = 0.380) for the CDK6−Vcyclin−aminopurvalanol complex. A model of the inhibitor aminopurvalanol was created by modification of purvalanol B from the CDK2−purvalanol B complex structure (PDB code 1CKP). The initial CNS topology, restraints, and coordinates for PD0332991 were obtained using the ligand builder module in PHENIX.[30] The models were refined using alternate cycles of automated refinement in CNS[31] and Refmac5.0[22] and manual rebuilding in O.[32] Final model statistics are listed in Table 1. The Ramachandran plot for both complex structures shows one residue, V181, in a disallowed conformation. The equivalent residue, V164 in CDK2, was shown to adopt a similar unfavorable conformation, which confers a substrate specificity for Pro at the P + 1 position, following the phosphorylatable S/T residue in the substrate.[33] The lower quality of the Ramachandran plots otherwise is explained by the limited resolution of the structures and high-temperature factors especially in the N-terminal kinase domains. The coordinates and structure factors were submitted to the PDB data bank with ID code 2EUF for the CDK6−PD0332991 complex and code 2F2C for the complex with aminopurvalanol.

Structure Analysis. Protein−ligand interactions were determined with the program CONTACT.[22] CDKs were superimposed using the McLachlan algorithm[34] as implemented in the program ProFit,[35] using the C_α atoms of residues 98−163 of CDK6 and their homologues in other CDKs for superposition. Residues 98−163

were chosen for superposition because they encompass all the catalytic residues and 13 out of 15 contact residues in the CDK6−PD0332991 complex. By omission of the residues from the N-terminal domain and more variable parts of the C-terminal domain for superposition, the fit for the superimposed ligand binding sites becomes better, which is the relevant part of the CDK structures for this analysis.

Acknowledgment. We thank the laboratory of Prof. L. Meijer for performing inhibitor binding assays for the CDK6−Vcyclin complex with aminopurvalanol, and the staff at the ALS, Berkeley, CA, who provided excellent facilities for data collection. We are grateful to Dr. Peter L. Toogood of the Pfizer Global Research and Development, Michigan Laboratories, for providing a sample of PD0332991.

References

(1) Sielecki, T. M.; Boylan, J. F.; Benfield, P. A.; Trainor, G. L. Cyclin-dependent kinase inhibitors: useful targets in cell cycle regulation. *J. Med. Chem.* **2000**, *43*, 1−18.
(2) Blagden, S.; de Bono, J. Drugging cell cycle kinases in cancer therapy. *Curr. Drug Targets* **2005**, *6*, 325−335.
(3) Meijer, L.; Leclerc, S.; Leost, M. Properties and potential-applications of chemical inhibitors of cyclin-dependent kinases. *Pharmacol. Ther.* **1999**, *82*, 279−284.
(4) Senderowicz, A. M.; Sausville, E. A. Preclinical and clinical development of cyclin-dependent kinase modulators. *J. Natl. Cancer Inst.* **2000**, *92*, 376−387.
(5) Malumbres, M.; Barbacid, M. To cycle or not to cycle: a critical decision in cancer. *Nat. Rev. Cancer* **2001**, *1*, 222−231.
(6) Garrett, M. D.; Fattaey, A. CDK inhibition and cancer therapy. *Curr. Opin. Genet. Dev.* **1999**, *9*, 104−111.
(7) Carnero, A. Targeting the cell cycle for cancer therapy. *Br. J. Cancer* **2002**, *87*, 129−133.
(8) Lundberg, A. S. Weinberg, R. A. Functional inactivation of the retinoblastoma protein requires sequential modification by at least two distinct cyclin−cdk complexes. *Mol. Cell. Biol.* **1998**, *18*, 753−761.
(9) Chen, Q.; Jin, J.; Jinno, S.; Okayama, H. Overexpression of Cdk6−cyclin D3 highly sensitizes cells to physical and chemical transformation. *Oncogene* **2003**, *22*, 992−1001.
(10) Meyerson, M.; Harlow, E. Identification of G1 kinase acticity for cdk6, a novel cyclin D partner. *Mol. Cell. Biol.***1994**, *14*, 2077−2086.
(11) Sellers, W. R. Kaelin, W. G. Role of the retinoblastoma protein in the pathogenesis of human cancer. *J. Clin. Oncol.* **1997**, *15*, 3301−3312.
(12) Kaelin, W. G. J. Alterations in G1-S cell-cycle control contributing to carcinogenesis. *Ann. N. Y. Acad. Sci.* **1997**, *833*, 29−33.
(13) Bartek, J.; Lukas, J.; Bartkova, J. Perspective: defects in cell cycle control and cancer. *J. Pathol.* **1999**, *187*, 95−99.
(14) Hall, M.; Peters, G. Genetic alterations of cyclin, cyclin-dependent kinases, and cdk inhibitors in human cancer. *Adv. Cancer Res.* **1996**, *68*, 67−108.
(15) Soni, R.; O'Reilly, T.; Furet, P.; Muller, L.; Stephan, C.; Zumstein-Mecker, S.; Fretz, H.; Fabbro, D.; Chaudhuri, B. Selective in vivo and in vitro effects of a small molecule inhibitor of cyclin-dependent kinase 4. *J. Natl. Cancer Inst.* **2001**, *93*, 436−446.
(16) Toogood, P. L.; Harvey, P. J.; Repine, J. T.; Sheehan, D. J.; VanderWel, S. N.; Zhou, H.; Keller, P. R.; McNamara, D. J.; Sherry, D.; Zhu, T.; Brodfuehrer, J.; Choi, C.; Barvian, M. R.; Fry, D. W. Discovery of a potent and selective inhibitor of cyclin-dependent kinase 4/6. *J. Med. Chem.* **2005**, *48*, 2388−2406.
(17) VanderWel, S. N.; Harvey, P. J.; McNamara, D. J.; Repine, J. T.; Keller, P. R.; Quin, J., 3rd; Booth, R. J.; Elliott, W. L.; Dobrusin, E. M.; Fry, D. W.; Toogood, P. L. Pyrido[2,3-*d*]pyrimidin-7-ones as specific inhibitors of cyclin-dependent kinase 4. *J. Med. Chem.* **2005**, *48*, 2371−2387.
(18) Fry, D. W.; Harvey, P. J.; Keller, P. R.; Elliott, W. L.; Meade, M.; Trachet, E.; Albassam, M.; Zheng, X.; Leopold, W. R.; Pryer, N. K.; Toogood, P. L. Specific inhibition of cyclin-dependent kinase 4/6 by PD 0332991 and associated antitumor activity in human tumor xenografts. *Mol. Cancer Ther.* **2004**, *3*, 1427−1438.
(19) Lu, H.; Chang, D. J.; Baratte, B.; Meijer, L.; Schulze-Gahmen, U. Crystal structure of a human cyclin-dependent kinase 6 complex with a flavonol inhibitor, fisetin. *J. Med. Chem.* **2005**, *48*, 737−743.
(20) Rosania, G. R.; Merlie, J., Jr.; Gray, N.; Chang, Y. T.; Schultz, P. G.; Heald, R. A cyclin-dependent kinase inhibitor inducing cancer cell differentiation: biochemical identification using Xenopus egg extracts. *Proc. Natl. Acad. Sci. U.S.A.* **1999**, *96*, 4797−4802.
(21) Schulze-Gahmen, U.; Kim, S. H. Structural basis for CDK6 activation by a virus-encoded cyclin. *Nat. Struct. Biol.* **2002**, *9*, 177−181.
(22) Collaborative Computational Project, Number 4. The CCP4 suite: programs for protein crystallography. *Acta Crystallogr. D* **1994**, *50*, 760−763.
(23) Davies, T. G.; Pratt, D. J.; Endicott, J. A.; Johnson, L. N.; Noble, M. E. Structure-based design of cyclin-dependent kinase inhibitors. *Pharmacol. Ther.* **2002**, *93*, 125−133.
(24) Honma, T.; Yoshizumi, T.; Hashimoto, N.; Hayashi, K.; Kawanishi, N.; Fukasawa, K.; Takaki, T.; Ikeura, C.; Ikuta, M.; Suzuki-Takahashi, I.; Hayama, T.; Nishimura, S.; Morishima, H. A novel approach for the development of selective Cdk4 inhibitors: library design based on locations of Cdk4 specific amino acid residues. *J. Med. Chem.* **2001**, *44*, 4628−4640.
(25) Gray, N. S.; Wodicka, L.; Thunnissen, A. M.; Norman, T. C.; Kwon, S.; Espinoza, F. H.; Morgan, D. O.; Barnes, G.; LeClerc, S.; Meijer, L.; Kim, S. H.; Lockhart, D. J.; Schultz, P. G. Exploiting chemical libraries, structure, and genomics in the search for kinase inhibitors. *Science* **1998**, *281*, 533−538.
(26) VanderWel, S. N.; Harvey, P. J.; McNamara, D. J.; Repine, J. T.; Keller, P. R.; Quin, J., 3rd; Booth, R. J.; Elliott, W. L.; Dobrusin, E. M.; Fry, D. W.; Toogood, P. L. Pyrido[2,3-*d*]pyrimidin-7-ones as specific inhibitors of cyclin-dependent kinase 4. *J. Med. Chem.* **2005**, *48*, 2371−2387.
(27) Schulze-Gahmen, U.; Kim, S. H. Crystallization of a complex between human CDK6 and a virus-encoded cyclin is critically dependent on the addition of small charged organic molecules. *Acta Crystallogr., Sect. D: Biol. Crystallogr.* **2001**, *57*, 1287−1289.
(28) Otwinowski, Z.; Minor, W. Processing of X-ray diffraction data collected in oscillation mode. *Methods Enzymol.* **1997**, *276*, 307−326.
(29) Navaza, J. AMoRe: an automated package for molecular replacement. *Acta Crystallogr. A* **1994**, *50*, 157−163.
(30) Adams, P. D.; Gopal, K.; Grosse-Kunstleve, R. W.; Hung, L. W.; Ioerger, T. R.; McCoy, A. J.; Moriarty, N. W.; Pai, R. K.; Read, R. J.; Romo, T. D.; Sacchettini, J. C.; Sauter, N. K.; Storoni, L. C.; Terwilliger, T. C. Recent developments in the PHENIX software for automated crystallographic structure determination. *J. Synchrotron Radiat.* **2004**, *11*, 53−55.
(31) Brunger, A. T.; Adams, P. D.; Clore, G. M.; DeLano, W. L.; Grosse-Kunstleve, R. W.; Jiang, J. S.; Kuszewski, J.; Nilges, M.; Pannu, N. S.; Read, R. J.; Rice, L. M.; Simonson, T.; Warren, G. L. Crystallography & NMR system: A new software suite for macromolecular structure determination. *Acta Crystallogr. D* **1998**, *54*, 905−921.
(32) Jones, T. A.; Zou, J. Y.; Cowan, S. W.; Kjelgaard, M. Improved methods for building protein models in electron density maps and the location of errors in these models. *Acta Crystallogr. A* **1991**, *47*, 110−119.
(33) Brown, N. R.; Noble, M. E. M.; Endicott, J. A.; Johnson, L. N. The structural basis for specificity of substrate and recruitment peptides for cyclin-dependent kinases. *Nat, Cell Biol.* **1999**, *1*, 438−443.
(34) McLachlan, A. D. Rapid comparison of protein structures. *Acta Crystallogr. A* **1982**, *38*, 871−873.
(35) Martin, A. C. R. http://www.bioinf.org.uk/software/profit.
(36) DeLano, W. L. *The PyMOL Molecular Graphics System*; DeLano Scientific: San Carlos, CA, 2002; http://www.pymol.org.

JM0600388